Inverse Design of Nanoparticles Using Multi-Target Machine Learning

Sichao Li and Amanda S. Barnard*

In this study a new approach to inverse design is presented that draws on the multi-functionality of nanomaterials and uses sets of properties to predict a unique nanoparticle structure. This approach involves multi-target regression and uses a precursory forward structure/property prediction to focus the model on the most important characteristics before inverting the problem and simultaneously predicting multiple structural features of a single nanoparticle. The workflow is general, as demonstrated on two nanoparticle data sets, and can rapidly predict property/structure relationships to guide further research and development without the need for additional optimization or high-throughput sampling.

1. Introduction

Inverse design[1–3] that prescribes a structure is a primary objective in materials informatics, and the ultimate goal of much academic and industrial research, but the majority of materials informatics uses machine learning (ML) to make forward predictions of a property of a material (the target label) based on the structural characteristics (the features). These are referred to as structure/property relationships, and they are used to inform synthesis and processing strategies; both real and hypothetical.[1,2,4–6] If a scientist or engineer makes a particular type of material (chemical composition, lattice type, defect configuration, etc) then these structure/property relationships predict what properties they can expect.[7–9] Inverse design, however, involves inverted property/structure relationships, and are highly desirable since a researcher usually knows what properties they need for a particular application and want a "recipe" of what they should be attempting to make in the lab. Inverse design is more complicated in nanomaterials design, where the finite

sizes and multitude of shapes mean the design space is larger.[10]

This topic has been approached in the past using interpretable structure/property relationships generated with machine learning methods that expose attributes such as feature importance profiles that rank the structural features by how influential they are in the model, together with the assumption that the features are equally influential in determining the structure/property relationship that the model represents. This is not necessarily the case, and also fails to eliminate the undesirable need to make, or model, a large number of materials to see which particular values of these important structural features produce the desired result. In addition to exhaustive sampling and an additional step to optimize the outcomes, this approach also suffers from too much specificity. Structure/property relationships typically involve many structural features but only one target property label. This makes inverting the problem difficult as there will be only one known variable (property) and numerous unknown variables (structures) making the solution intractable.

An alternative approach to inverse design is possible in cases where more than one property label is known. Multi-functional materials have been receiving considerable attention in material science as they provide a greater opportunity for tuning the material to a particular application, and lower the cost of devices by reducing the need for multiple components. If enough labels are available, we can invert the problem and use the properties as inputs to predict a target structural characteristics. This mitigates the issue of having insufficient known variables to predict an unknown structure, making a mapping tractable, and the fact that one structural characteristic may be not be sufficient to guide experiments. In some cases a single structural characteristic might be enough, such as the strongly size-dependent optical emission of quantum dots, but in many cases the underlying structure/property relationships are more complicated and so the property/structure relationship will not be useful unless we can extract a more holistic structural profile.

In this paper we design and demonstrate a new inverse design workflow using multi-target random forest regressors, and test it on two data sets originally generated using electronic structure simulations. As we will show, by informing the inverse models with information on the important structural characteristics in a conventional (forward) structure/property relationship, new property/structure relationships can be predicted with comparable performance in terms of accuracy and generalizability.

S. Li, A. S. Barnard
School of Computing
Australian National University
Acton, Australian Capital Territory 2601, Australia
E-mail: amanda.s.barnard@anu.edu.au

The ORCID identification number(s) for the author(s) of this article can be found under https://doi.org/10.1002/adts.202100414

**ADVANCED
SCIENCE NEWS**

www.advancedsciencenews.com

**ADVANCED
THEORY AND
SIMULATIONS**

www.advtheorysimul.com

2. Experimental Section

2.1. Data Sets

This study employed two publicly available ensemble data sets of 500 diamond nanoparticles[11,12] and 425 silver nanoparticles,[13] respectively. Both of the data sets were originally simulated using electronic structure methods and characterized numerically using statistical analysis to define structural features and electron transfer properties.[14–16] The structural features are defined in Tables S1 and S2, Supporting Information. Feature extraction was not conducted as part of this study, and information on how the features were generated can be obtained from references listed on the data repository.

Feature selection and engineering play an important role in the application of machine learning in material science,[17] and influence model performance. Ghiringhelli et al.[18] systematically extracted the important features for the energy difference of zinc blende or wurtzite and rocksalt semiconductors to improve model performance. Constant features should be ignored, and irrelevant (or minimally relevant) features should be avoided by filtering based on the standard deviation of each feature, as they contributed nothing to the accuracy of classification and regression. Similarly, strongly correlated features were redundant as they both contributed the same information during learning, and unnecessarily complicated the model by introducing bias that should be reduced. In the study, linearly correlated features were identified using a correlation matrix and features with over 95% correlation were removed, and features with a standard deviation of less than 0.1% were eliminated to reduce noise. Once the feature set has been cleaned, the remaining set can be recursively optimized until the most informative features were retained as described below. In the study, the feature selection was achieved based on the Gini importance of random forests.[19]

The labels included in the two data sets were slightly different, but both contained electron charge transfer properties and a measure of thermodynamic stability. This included the formation energy (Formation_E) and thermodynamic probability of observation (Probability) originally calculated using a Boltzmann distribution and the free energy different at 300 K at atmospheric pressure.[20] The electron change transfer properties included the ionization potential (IP), the electron affinity (EA), the electronic band gap (EG), the electronegativity (EN), or the energy the Fermi level (EF), all measured in eV. Labeling was not conducted as part of this study, and information on how the labeling was conducted can be obtained from references listed on the data repository.

2.2. Multi-Target Random Forest Regression

The selection of the machine learning algorithm has been informed by the high-dimensional numerical target labels, which require a multi-target regression model. Borchani et al.[3,21] categorized existing methods for multi-output regression into problem transformation methods and algorithm adaptation methods. Problem transformation methods transform the multi-output problem into independent single-output problems, while algorithm adaptation methods involved the modification of specific existing single output methods making it suitable to directly handle multi-output data sets directly.[22] Algorithm adaptation methods, such as support vector machine (SVM) and regression trees, are more appropriate to this study due to the interpretability of feature importance, which was important for inverse design.[23] Tree-based methods were chosen over others as a nonparametric explanatory approach, making no assumption on the distribution of data and the structure of the model, provided excellent performance over alternatives.[24] Alternative interpretable adaptation methods would also be suitable.

A decision tree is a flowchart-like structure for a classification or regression process branching from the root node to leaf nodes that represent the discretized outcomes, passing through the internal nodes that classify each attribute.[25] Decision trees can intrinsically handle multi-task problems as the leaf nodes can refer to any collection of relevant classes. Random forest (RF)[26] is an ensemble technique that aggregates a large number of decision trees through bootstrap aggregation, also known as bagging,[27] and random feature selection methods.[28] Each decision tree in the forest is trained on a different data sample with random subsets of features, and "votes" determine the prediction that best resembles the limited scope at the point of prediction. RFs count each vote from individual trees and return the outputs with the most votes as the final ensemble prediction;[29] either the classes for classification or the mean prediction for regression. The feature selection criterion for internal nodes is the Gini impurity or information gain for classification and variance reduction for regression.[30] This approach increases the diversity amongst the ensemble members and avoids over-fitting, resulting in accurate decision forests. A RF ensemble predictor can be extended to tackle multi-target learning problems by replacing the typical univariate trees in the RF with multivariate trees,[31–33] making it ideal for the present study.

This is distinct from other approaches that share information such as transfer learning. Transfer learning aims to achieve high performance by transferring knowledge from the source task, while multi-target learning learns the target and the source task simultaneously. Transfer learning focused on sequential sharing knowledge/representations between targets, using domain adaptation, where the targets have different data sources (even if the feature attributes are the same). Information about the structure of a similar model trained on a different source is transferred, but the new model is still trained on its own data. Multi-target learning is a parallel process, where a model is jointly trained to minimize several loss functions on different targets, using the same source data. This builds a representation that is useful for several problems, while exploiting commonalities and differences across tasks, but knowledge of the model structure is not transferred.

Another advantage is the ability to calculate the relative importance of each feature in a decision tree and random forests, and features that contribute the most to predicting the target property can be identified by recursive feature elimination (RFE). As will be seen, this was extremely important in the present study as there was a limited number of property labels, and therefore a limited number of structural characteristics that can be reliably predicted. For each feature on a decision tree, the importance was calculated as the decrease in the impurity of the split weighted by the probability of arriving that node, which was the number of samples that arrived at the node, divided by the total number of
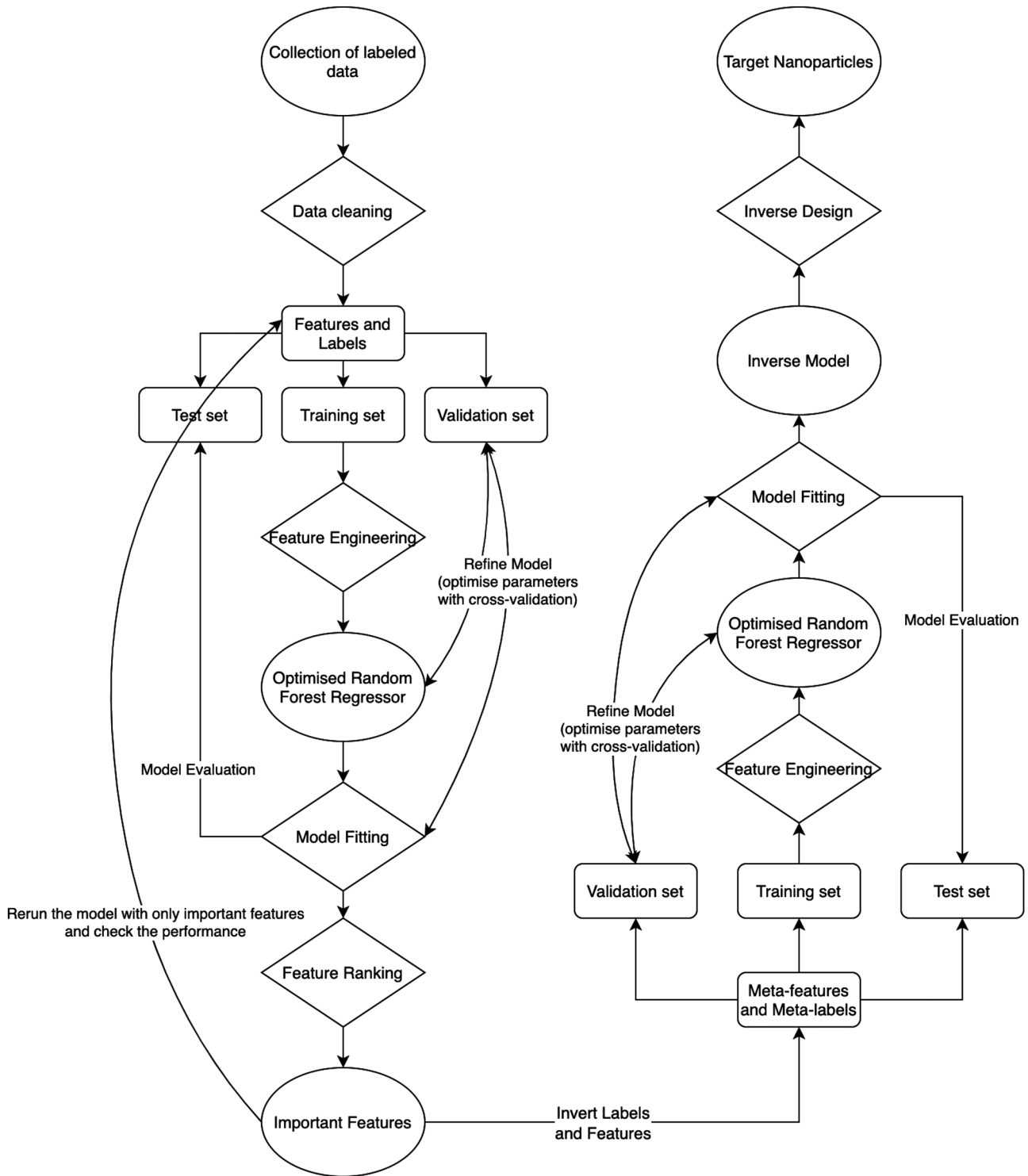
**ADVANCED
SCIENCE NEWS**

www.advancedsciencenews.com

**ADVANCED
THEORY AND
SIMULATIONS**

www.advtheorysimul.com

Figure 1. Inverse design workflow.

samples, from which features were ranked based on the averaged impurity over all trees in the forest.[34] The outcome is a ranked feature importance profile (histogram) and a prediction of the optimal number of features required to archive convergence of the cross validation score.

2.3. Workflow

To obtain a reliable inverse model, the workflow is illustrated in **Figure 1**. Given the raw data set, preprocessing was undertaken to exclude outliers, standardize and normalize the features, and

2100414 (3 of 12)

**ADVANCED
SCIENCE NEWS**

www.advancedsciencenews.com

**ADVANCED
THEORY AND
SIMULATIONS**

www.advtheorysimul.com

split the data sets to training, testing, and validation sets. This process was accompanied by the selection of a machine learning model that was suitable for the multi-target regression; in this case RF. To begin the forward RF model was optimized and trained using *k*-fold cross validation, which enabled the regressor to rank the features by Gini importance. Recursive feature elimination was used to select the most important features sufficient for the model to simultaneously predict the property labels without loss of accuracy or generalizability. This was important to reduce the number of predictable structural characteristics to be commensurate with (or similar to) the number of available properties, and while not essential, it was good practice to repeat the forward model optimization and training using only the final subset of features to quantify any loss. The data set was then inverted; the reduced set of important features becoming structural "meta-labels," and the multiple property labels becoming the new "meta-features." The inverted set was then split into training, testing, and validation sets, and the optimization, training, and validating processes of the multi-target RF model was repeated. The forward model and the inverse model used the same inputs and targets, but in reverse. Once inverse training was complete, the inverse model was ready to be used.

3. Results

Before conducting experiments, each data set used herein was cleaned to remove linearly correlated features and noise, then scaled using the MinMax scaler and normalized (both features and labels). In the case of the pairs of features that are linearly correlated (see correlation matrices in Supporting Information) we routinely retain the features that provide the greatest opportunity for experimental control, or the greatest experimental interpretability. The retained features are highlighted in the lists in Supporting Information. Following cleaning the data sets were split into 80% training set and 20% testing set prior to optimization. The same train/test split, with the same random seed, was used for all models (both forward and inverse). For each regressor we defined a grid of hyper-parameter ranges and searched 1000 random combination of values sampled from the grid, performing five-fold cross validation at each iteration. All optimized regressors were trained with ten-fold cross validation. The accuracy and generalizability of all of the hyper-parameters-tuned models was assessed using the mean square error (MSE) and the mean absolute error (MAE) to evaluate the training, testing and cross-validation scores.[35] These results are tabulated, or included in learning curves which also quantify any under-fitting or over-fitting.

3.1. Nanodiamond

To investigate this approach to inverse design we have begun with the nanodiamond data set, as this is an experimentally and industrially relevant material that has promising applications in biotechnology and medicine.[36–41]

3.1.1. Forward Prediction

Cleaning of this data set (described above) resulted 16 structural features, `H_conc`, `HCP_conc`, `FCC_conc`, `F_111`, `F_110`, `F_100`,

Table 1. Forward predictions using the multi-target regression model of diamond nanoparticles, with all of the structural features retained after data cleaning, or the top nine important features identified using recursive feature elimination. The results are evaluated using the mean absolute error (MAE), the mean square error (MSE), and the root mean square error (RMSE).

Prediction	Feature set (number)	Target (number)	MAE	MSE	RMSE
Forward	Retained (16)	All (5)	0.034	0.003	0.053
Forward	Important (9)	All (5)	0.035	0.003	0.057
Forward	Retained (16)	Probability (1)	0.021	0.001	0.034
Forward	Retained (16)	IP (1)	0.055	0.011	0.103
Forward	Retained (16)	EA (1)	0.041	0.005	0.073
Forward	Retained (16)	EG (1)	0.039	0.005	0.072
Forward	Retained (16)	EN (1)	0.045	0.006	0.077

`Sphericity`, `CC_coord`, `sp1`, `sp2`, `sp2x`, `dCC`, `dCCe`, `aCCC`, `aCCCe`, and `D_nm`, remaining in the feature space.

The forward multi-target prediction was first trained with all 16 features to predict the `Probability`, `EN`, `IP`, `EA`, and `EG` property labels simultaneously, achieving low testing errors, as shown in **Table 1**. The feature importance, based on Gini impurity, is ranked in **Figure 2**a. The training process, combined with cross validation is visualized in the learning curve in Figure 2b, where we can see convergence with respect to the number of training instances has been achieved, leaving only minor over-fitting and no under-fitting. As shown in the recursive feature elimination profile in Figure 2c the model performance is maximized when the nine important features are selected (in order of importance: `sp2x`, `H_conc`, `sp2`, `dCCe`, `aCCCe`, `D_nm`, `aCCC`, `FCC_conc`, `CC_coord`), so the forward model was reoptimized and trained using this subset. Overall these results are consistent with previously reported regression studies of this data set, even though they used different regressors (gradient boosting and extra trees[14]). The results using the important subset are shown in Figure 2d and Table 1.

As we can see by comparing these results there is almost no loss of accuracy or generalizablity, and no introduction of under-fitting or additional over-fitting, when using the important subset of features; the five target properties can be reliably predicted using only the top nine structural features. This is computationally convenient, but also scientifically important since the size (`D_nm`) and hydrogen concentration (`H_conc`) are based on inputs that can in principle be controlled directly, and the speciation (`sp2`, `sp2x`) and lattice structure (`FCC_conc`, `CC_coord`) can be tuned indirectly in the lab. These results also compare well to the individual single-target RF models optimized and trained using all retained features to predict each nanodiamond property, as shown in Table 1.

3.1.2. Inverse Prediction

As indicated in the workflow diagram, multi-target regression was then used to train the inverse property/structure model using the reduced data set which contains nine most important structural characteristics and five nanodiamond properties. The RF algorithm was reoptimized and retrained with the five prop-
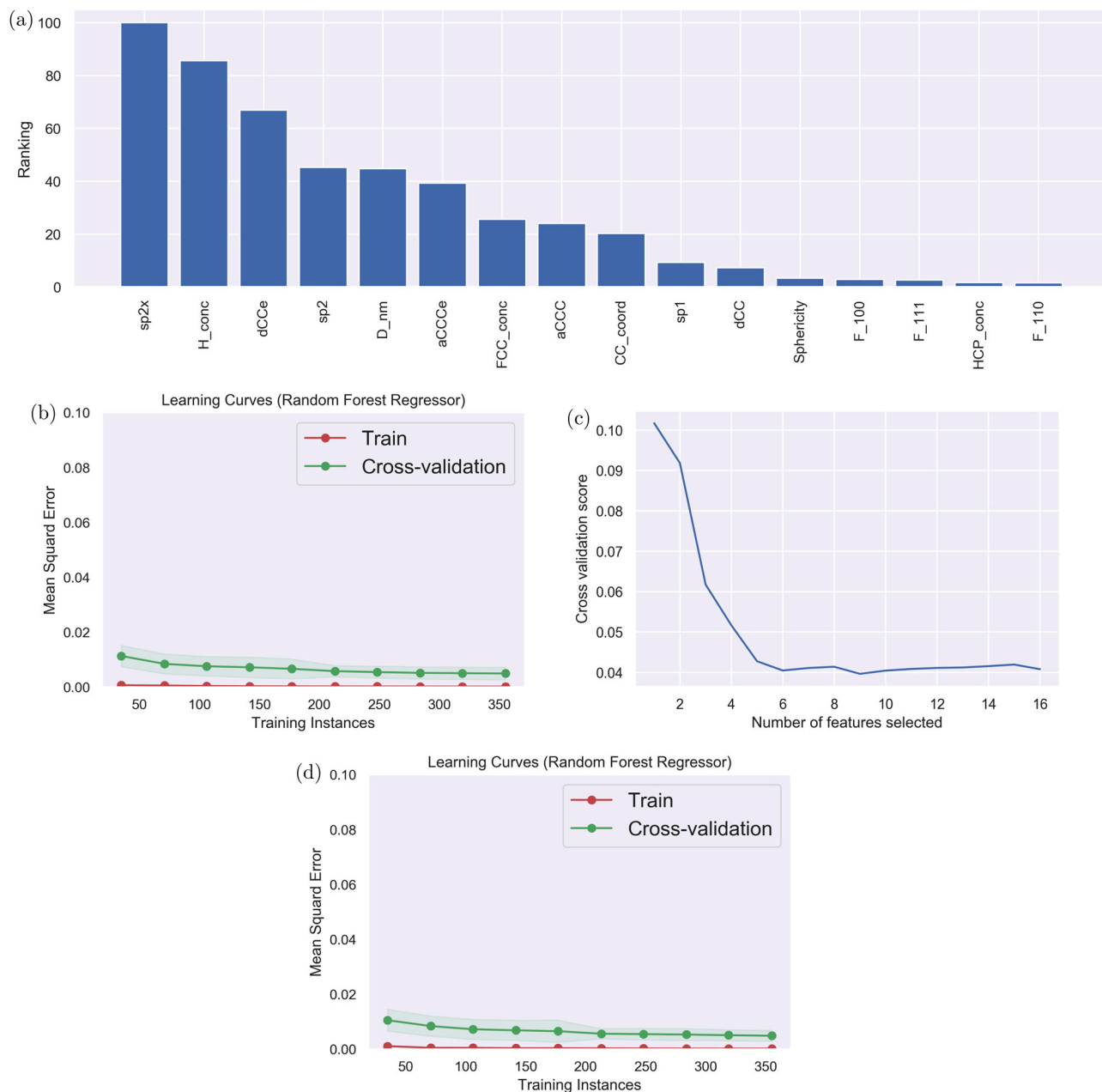
ADVANCED
SCIENCE NEWS
www.advancedsciencenews.com

ADVANCED
THEORY AND
SIMULATIONS
www.advtheorysimul.com

Figure 2. Results for the forward multi-target regression simultaneously predicting all five target properties of the nanodiamonds trained on 16 structural features retained after data cleaning, including a) the feature importance profile rankings, b) the learning curve showing the accuracy and generalizablity, c) results of recursive feature elimination showing optimal results can be achieved with nine features, and d) the learning curve for forward prediction using only the nine optimal, high ranking important features, showing no loss of accuracy or generalizablity.

erties becoming "meta-features" and the nine structural features becoming "meta-labels." In the case of the inverse prediction, training with all five meta-features was undertaken to predict the `Probability`, `EN`, `IP`, `EA`, and `EG` meta-labels simultaneously, achieving low errors, as shown in **Table 2**. We can see from this table by comparing results for the multi-target inverse prediction and the single-target inverse prediction that the quality is similar if all or one of the structural meta-labels is predicted from the properties, and that the ranking of the meta-label in the forward model (where it was a feature) does not correlate to the MAE or

MSE in the inverse model. We can also see by comparing Tables 1 with 2 that the quality of the predictions are similar, based on the MAE and MSE, suggesting that the performance of a forward model is a reasonable indicator of the expected performance of the inverse model. The learning curves to accompany the single-target inverse predictions summarized in Table 2 are provided in Supporting Information.

All learning curves for multi-target inverse models using different numbers of meta-features and meta-labels are shown in **Figure 3**, where we can see that any reduction of the num-

2100414 (5 of 12)

Table 2. Inverse predictions using the multi-target regression model, with all of the property meta-features or the four electronic meta-features (omitting the probability of observation), predicting all of the important meta-label, a subset of the six meta-labels or each meta-label individually. The structural meta-labels are listed in order of importance in the forward model. The results are evaluated using the mean absolute error (MAE), the mean square error (MSE) and the root mean square error (RMSE).

Prediction	Feature set (number)	Target (number)	MAE	MSE	RMSE
Inverse	All (5)	All (9)	0.047	0.010	0.091
Inverse	Electronic (4)	All (9)	0.053	0.012	0.105
Inverse	All (5)	Subset (6)	0.052	0.012	0.101
Inverse	Electronic (4)	Subset (6)	0.060	0.015	0.120
Inverse	All (5)	sp2x (1)	0.050	0.012	0.109
Inverse	All (5)	H_conc (1)	0.027	0.005	0.072
Inverse	All (5)	dCCe (1)	0.019	0.001	0.031
Inverse	All (5)	sp2 (1)	0.061	0.017	0.129
Inverse	All (5)	D_nm (1)	0.014	0.001	0.022
Inverse	All (5)	aCCCe (1)	0.041	0.005	0.073
Inverse	All (5)	FCC_conc (1)	0.067	0.010	0.100
Inverse	All (5)	aCCC (1)	0.049	0.0103=	0.1013=
Inverse	All (5)	CC_coord (1)	0.0712=	0.018	0.134

ber of meta-features or meta-labels used in the inverse model increases the over-fitting, though only slightly. The inverse model exhibits high accuracy and generalizability and remarkable resilience to minor changes in the number of properties available and structural characteristics which need to be predicted.

Two questions arise from outcome: would the method still work if less than five properties were available, and can the results be improved if the number of target structural characteristics was closer to the number of available properties? To test the former we omitted the probability of observation, as it is difficult to obtain experimentally, and retrained the inverse model to predict the structural meta-labels with only the electronic meta-features IP, EA, EG, and EN. We can see from Table 2 that the loss of performance is in the third decimal place, indicating that more properties are desirable but the impact of having more or less of them is marginal. In the latter case we used all meta-features and the subset of electronic meta-features to predict the six meta-labels that can be potentially tuned in the lab: sp2x, H_conc, sp2 and D_nm, FCC_conc, and CC_coord. These all relate in some way to the size and the surface structure (surface chemistry and reconstructions). Here we can see that the loss in performance when using fewer structural meta-labels is also less than 1%, indicat-
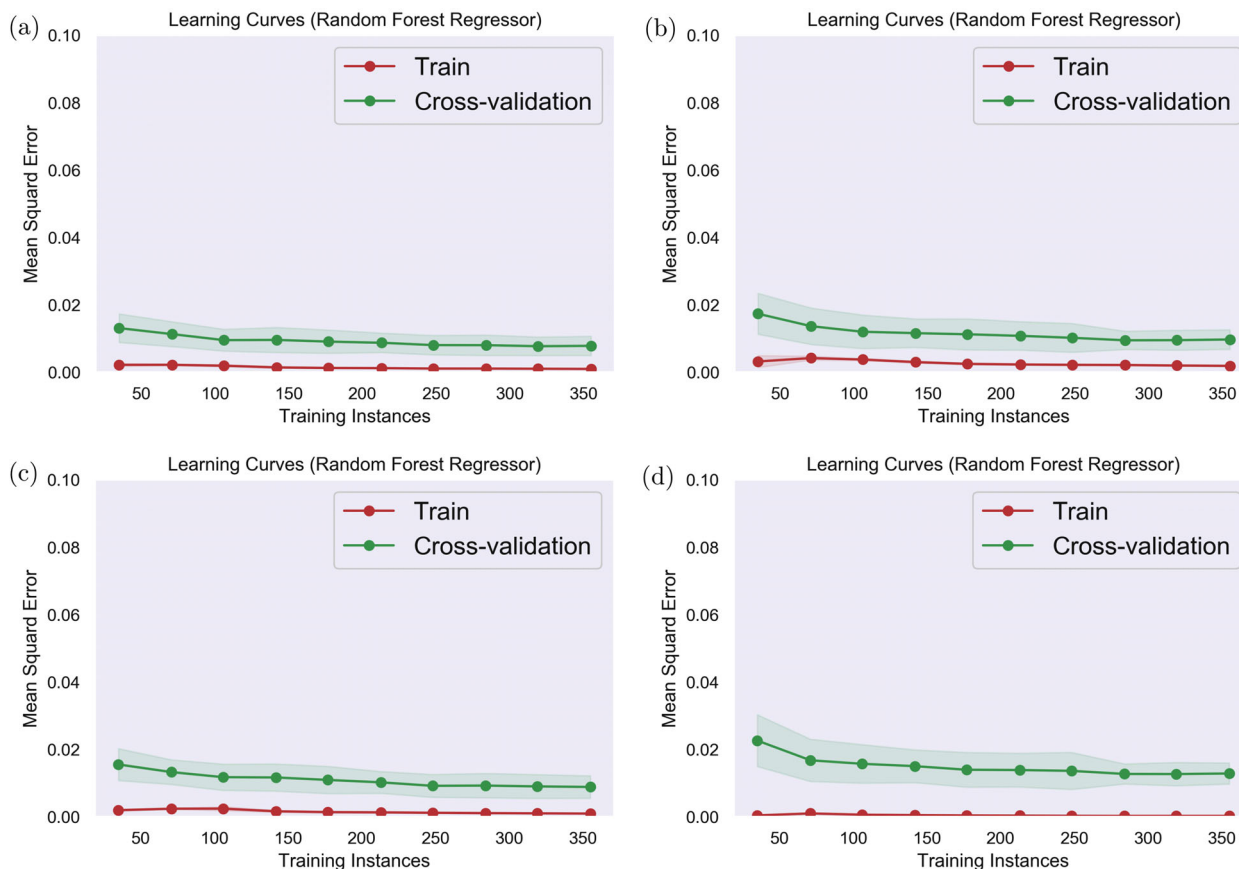

Figure 3. Learning curves for different combinations of inputs in the multi-target inverse model predicting using 500 nanodiamonds including a) five property meta-features predicting nine structural meta-labels, b) four property meta-features predicting nine structural meta-labels, removing Probability that is difficult to obtain experimentally, leaving only electronic meta-features (IP, EA, EG, and EN), c) five property meta-features predicting 6 structural meta-labels, representing the top ranking structural characteristics from the forward model (sp2x, H_conc, sp2 and D_nm, FCC_conc, and CC_coord), and d) four property meta-features predicting 6 structural meta-labels. The testing results are evaluated using the mean square error (MSE).

Table 3. Forward predictions using the multi-target regression model of silver nanoparticles, with all of the structural features retained after data cleaning, or the top four important features identified using recursive feature elimination. The testing results are evaluated using the mean absolute error (MAE), the mean square error (MSE), and the root mean square error (RMSE).

Prediction	Feature set (number)	Target (number)	MAE	MSE	RMSE
Forward	Retained (48)	All (5)	0.061	0.009	0.081
Forward	Important (4)	All (5)	0.071	0.012	0.094
Forward	Retained (48)	Formation_E (1)	0.025	0.001	0.033
Forward	Retained (48)	IP (1)	0.095	0.015	0.123
Forward	Retained (48)	EA (1)	0.058	0.006	0.078
Forward	Retained (48)	EG (1)	0.034	0.003	0.052
Forward	Retained (48)	EF (1)	0.149	0.039	0.196

ing that there is little cost to focusing on structural characteristics that represent possible inputs for experiments, provided they are highly ranked.

3.2. Silver Nanoparticles

To ensure the feasibility of the workflow, and to test if this inverse design strategy is general, we have repeated this entire process on the data set of silver nanoparticles (described above) using identical steps. During data cleaning the silver data set required the removal of some outliers, retaining instances where IP<5 eV, EA>2.5 eV, EG<2.5 eV, −4.05<EF<−3.5 eV and Formation_E<0.8 eV. This resulted in a final set of 414 nanoparticles.

3.2.1. Forward Prediction

The forward multi-target prediction training was initially conducted with 48 retained features following cleaning and five property labels: Formation_E, IP, EA, EG, and EF. The results for the MAE and MSE are provided in **Table 3**, and the learning curve in **Figure 4**a. The feature importance ranking is shown in Figure 4b, and the recursive feature elimination profile in Figure 4c reveal that an optimal model can be achieved using only four structural features: Ag_Ratio, R_avg, Anisotropy, and Facets. The results using this reduced feature set is provided in Table 3 showing minimal loss of performance, and the associated learning curve is shown in Figure 4d. Retraining the forward multi-target model with only important features once again reduced the performance by less than 1%, and the results of both models compare well with the associated single-target predictions, as shown in Table 3. The performance of the single-target prediction for the energy of the Fermi level (EF) is an obvious outlier, with larger errors than the others, which is consistent with previous results using this data set,[15] due to the bimodal distribution of this label.

3.2.2. Inverse Prediction

Once again the problem is inverted, and the five properties become meta-features and the four structural features become

meta-labels. The multi-target RF model is reoptimized and trained using the procedure above, and the results are provided in **Table 4** and **Figure 5**. In this case the number of facets (an indicator of the nanoparticle morphology) is a difficult label to predict, suggesting an alternative shape-dependent feature/meta-label may improve the outcome. All of the other single-target meta-labels perform similarly to the multi-target prediction. As above for nanodiamonds, we also reduced the number of meta-features, dropping the formation energy (which is difficult to measure experimentally) and reoptimized and trained the multi-target model. The results in Table 4 show an even smaller loss of performance than the nanodiamond predictions, with the MAE and MSE increasing by only ≈ 0.5%, and the learning curves in Figure 5b being virtually indistinguishable.

4. Discussion

The inverse models predicted here show remarkably good performance (with low MSE and MAE), comparable to forward models using the same reduced sets of important features, and single-target predictions. Although different accuracy metrics are available, since we are using a complicated and highly nonlinear regressor (multi-target random forest) the coefficient of determination (R^2) is inappropriate for interpreting dependent variability in our study.[42] Both MAE and MSE are practical in expressing the average model error, though MSE tends to penalizes large prediction errors. Using only one measurement is controversial,[43,44] so comparing both can provide a more comprehensive insight into the model performance. The limitation of evaluation using MSE and MAE is the absence of a standard and whether or not a MSE or MAE value is acceptable depends on the actual range of the target variable,[45] and the fault tolerance acceptable in a given application domain. In our study all of the data as standardized and normalized, so there is a consistent range and unit, but this is not enough for evaluation. For this reason, and for their intrinsic utility, the performance has been evaluated using learning curves. While a disadvantage of this multi-target regression is that the 45 degree plots typically used to compare the predicted and true values cannot be used for more than one target, learning curves for models offer the advantage of reporting both the training accuracy (including under-fitting) and generalizability (including over-fitting) via the cross-validation score, which is important since biased trees can be created if some classes dominate.[46,47]

Conventional 45 degree plots are not possible for multi-target regression, but we have provided explicit comparison of the predicted meta-labels against the ground truth of for three samples taken from the testing sets in Supporting Information. By comparing the results for nanodiamond case study and the silver nanoparticle case study we can see the silver model is superior, which can be partly attributed to the smaller number of metal-labels with respect to meta-features. This highlights the value of the feature selection provided by the forward models to reduce the dimensionality. It is entirely possible to use the L1 regularization to achieve this goal, but this has some disadvantages. Regularization consists of adding a penalty to different parameters of the model, such as the coefficients that multiply each of the predictors. L1 has the property of being able to shrink some of the coefficients to zero, effectively removing them from the model.
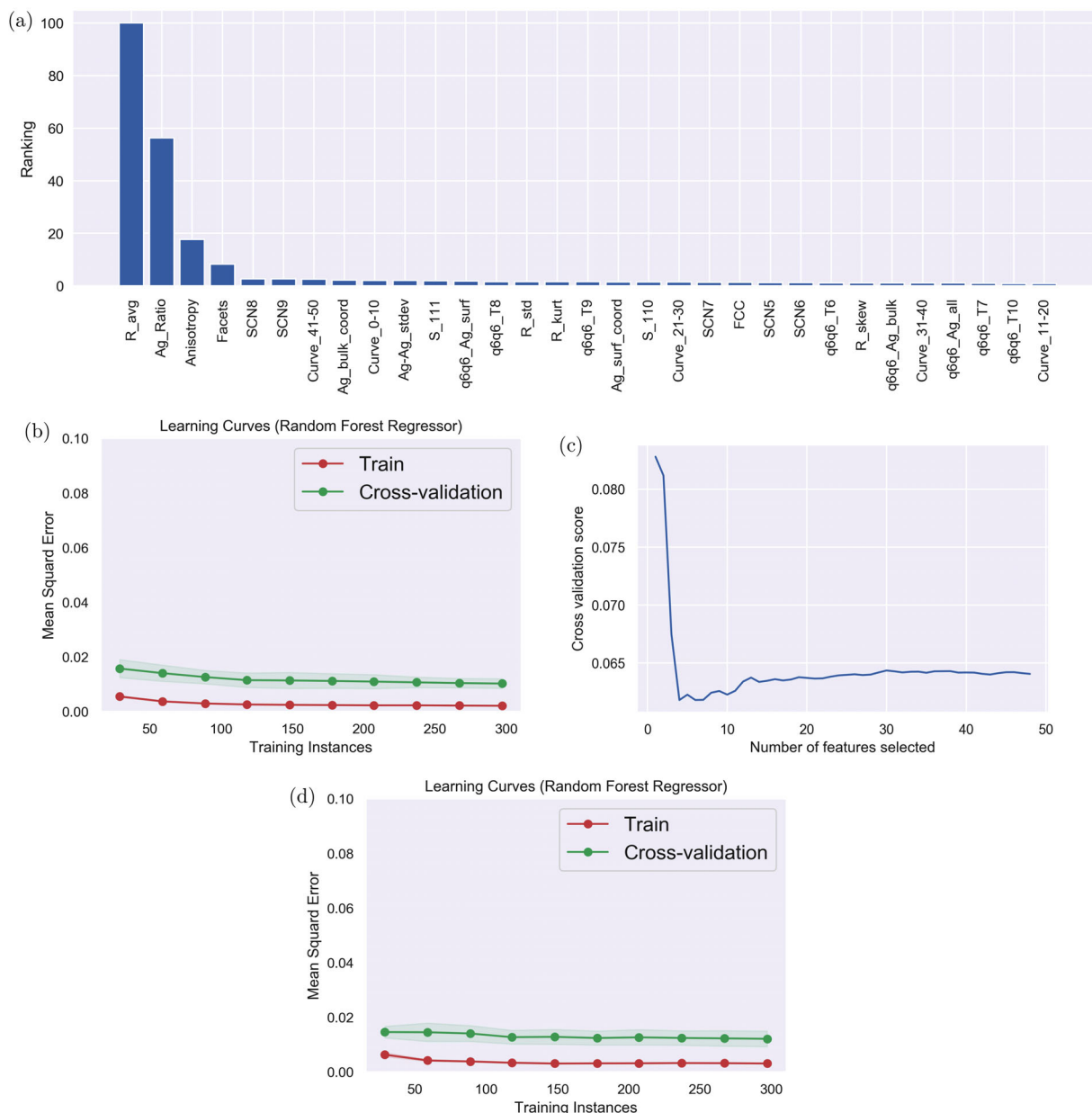
**ADVANCED
SCIENCE NEWS**

www.advancedsciencenews.com

**ADVANCED
THEORY AND
SIMULATIONS**

www.advtheorysimul.com

Figure 4. Results for the forward multi-target regression simultaneously predicting all five target properties of the silver nanoparticles trained on 48 structural features retained after data cleaning, including a) the feature importance profile rankings, b) the learning curve, c) results of recursive feature elimination showing optimal results can be achieved with four features, and d) the learning curve for forward prediction using only the four important features, showing no loss of accuracy and almost no loss of generalizablity. The testing results are evaluated using the mean square error (MSE).

While this reduces variance (improves generalizability), it can introduce bias (reducing accuracy) and there is no guarantee that the final feature set represents a reliable structure/property (or property/structure) relationship. A very important feature, such as the hydrogen concentration on the surface of nanodiamond or the average radius of silver, could contribute to the variance error because there is noise, while still being critical to the design of the nanoparticle. The backward elimination approach of recursive feature elimination prioritizes the important features that anchor the structure/property relationship, while still decreasing the dimensionality and maximizing the accuracy at the same time. This has some advantages in the context of nanomaterials design, but is not strictly the only way from a machine learning perspective. The disadvantage is that it necessitates training an optimized forward model before an inverse model is attempted, but this disadvantage is mitigated by the fact that a preview into the overall performance that can be expected from the inverse model can be obtained (though the forward model is likely to be superior).

Although the learning curves presented here indicate we have convergence with respect to the size of the training sets, it is likely that the results could be improved if more nanoparticle prop-

ADVANCED
SCIENCE NEWS
www.advancedsciencenews.com

ADVANCED
THEORY AND
SIMULATIONS
www.advtheorysimul.com

Table 4. Inverse predictions using the multi-target regression model for the silver nanoparticles, with all of the five property meta-features or the four electronic meta-features (omitting the formation energy), predicting all of the important meta-labels, and all meta-features predicting each meta-label individually. The structural meta-labels are listed in order of importance in the forward model. The testing results are evaluated using the mean absolute error (MAE), the mean square error (MSE), and the root mean square error (RMSE).

Prediction	Feature set (number)	Target (number)	MAE	MSE	RMSE
Inverse	All (5)	All (4)	0.073	0.021	0.119
Inverse	Electronic (4)	All (4)	0.079	0.023	0.125
Inverse	All (5)	Ag_Ratio (1)	0.021	0.003	0.057
Inverse	All (5)	R_avg (1)	0.017	0.001	0.027
Inverse	All (5)	Anisotropy (1)	0.091	0.021	0.146
Inverse	All (5)	Facets (1)	0.158	0.053	0.230

erties were available. To achieve a good result we recommend gathering as many properties as possible, and restricting the prediction to only the important structural characteristics, which should be identified using an entirely data-driven approach as we have done here (to help avoid evaluation bias). This step achieves a better balance in the number of known and unknown variables than an unrestricted multi-target model, reduces the computational complexity and the computation time. This approach also automatically ensures the inverse property/structure relationship remains close to the domain of applicability of the forward structure/property model. This reduces the likelihood of spurious correlations impacting the inverse model due to an inability to perfectly map insufficient meta-feature inputs to the meta-label outputs. However, if a very large number of properties are available it might also be worthwhile cleaning the labels by checking for correlations and noise as we have done for the original feature set, since they will eventually become meta-features. For example, in the case of the inverted predictions in the silver nanoparticle data set the correlation between Formation_E and EG is 97.4%, which would typically require one to be eliminated if they were among the original features. When

we did remove this label/meta-feature as there was small impact on the model performance, but removing too many properties (or retaining too many highly correlated properties) could have more significant consequences. In the present study we also preserved the original dimensions of the properties labels, since random forests are forgiving of data cleanliness and can perform well without standardization or normalization, but this might also be worth investigating if the number of properties is large.

Using these inverse models it is possible to input a list of desired properties and output a profile of the nanoparticle that would meet these requirements. An advantage of using multi-target regression is that one profile is given for one set of conditions, and there is no need to perform optimization to find a combination of structural characteristics that will work, though other authors have taken an optimization approach to inverse design. Tominaga et al. proposed an efficient procedure based on genetic algorithms (GAs) for optimization of a single inverse system.[48] Yang et al. also developed a package for inverse design, named IM²ODE (Inverse design of materials by multi-objective differential evolution), based on multi-objective differential evolution. Although the package implements structural optimization, and duplicate elimination to increase the efficiency, it is still an optimization method striving to solve a global searching task and is therefore time-consuming. As a result of using real-valued number instead of genes, differential evolution tends to be more effective than GAs, but maintaining a viable population of candidate solutions and low convergence properties are problematic.[49,50] Alternative approaches using evolutionary algorithms have been reported, but similarly suffer from poor scaling with respect to complexity and often require very expensive fitness functions for evaluation, often taking days to complete. The stopping criteria of genetic algorithms for predicting multi-targets is also unclear.[51]

Rather than using an evolutionary algorithm, Zunger et al. identified materials with specific functionalities using an inverse design framework based on a global searching task. High-throughput density functional theory calculations were used to discover highly efficient halide perovskites solar absorbers and high absorption thin-film photovoltaic materials.[52,53] The inverse band structure approach describe by the authors
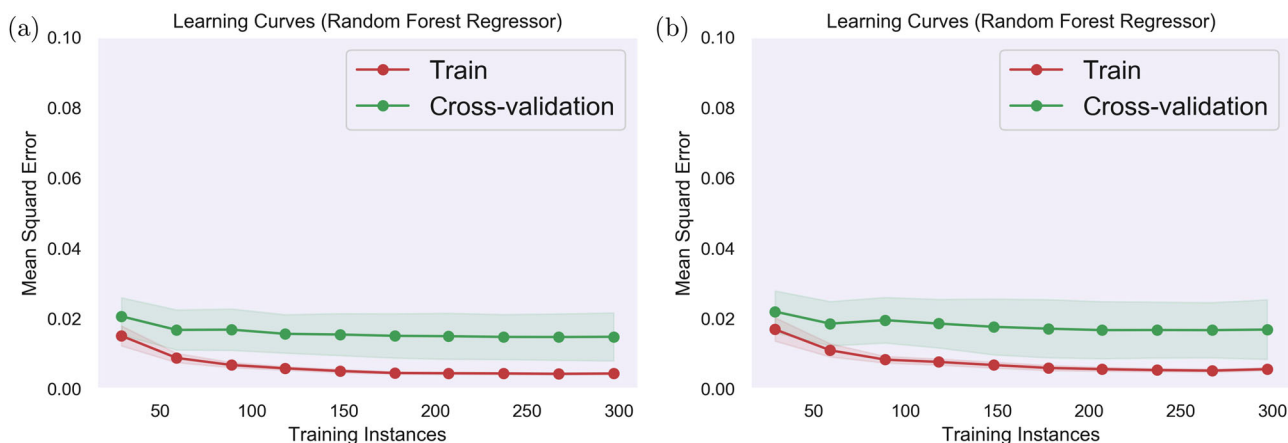

Figure 5. Learning curves for different the multi-target inverse model predicting using 414 silver nanoparticles including a) five property meta-features predicting four structural meta-labels, and b) four property meta-features predicting four structural meta-labels, removing Formation_E that is difficult to obtain experimentally, leaving only electronic meta-features (IP, EA, EG, and EF).

2100414 (9 of 12)

successfully identified atomic alloy configurations, using a linear-regression function to predict property/structure relationship,[54] but this approach suffers from the requirement of a comprehensive data set to enable a truly global search. As demonstrated in the study the collection of such a data set can be automated, but the reliability of such high-throughput systems depends on the number and types of competing candidate structures, and can result in impossible compounds.[1,55,56] Furthermore, not all property/structure relationships can be linearly regressed. In the present study we were able to employ a nonlinear regressor (RF) which does not rely on an external optimization method, or need an exhaustive data set, to be reliable. Traditional screening-based approaches can only choose from candidates that are in the data set,[57–59] whereas our method can identify configurations that are not in the data set. This could be advantageous in some circumstances. In general, a conventional forward-model-only screening approach has five mandatory steps: 1) train the forward model, 2) use the forward model to predict unknown instances, 3) rank the predicted outcomes, 4) apply screening criteria, 5) extract structural characteristics of acceptable materials. This process can be partially automated. Our approach has two mandatory steps since applying our model automatically outputs the structural characteristics: 1) train inverse model, 2) apply inverse model. This process can be entirely automated. Both approaches would benefit from the additional (optional) dimension reduction, as we have shown here, since both methods could result in a long list of characteristics that could be too difficult for researchers to use simultaneously. Ideally this dimension reduction should be focused, and interpretable, as we have demonstrated. Furthermore, the forward-only approach may also identify multiple acceptable candidates with no way of choosing between them (which could be useful, or could be a confusing), whereas our direct inverse approach identifies one acceptable candidate, thereby reducing ambiguity.

At this point it is worth highlighting that, while the data sets used here have significant diversity (distributions of sizes, mixtures of shapes, surface reconstructions, surface chemistry, twinning, etc), particularly the nanodiamond set that has different types of surface speciation, diversity does not necessarily introduce noise and other types nanomaterials data may be of lower quality due to factors such as measurement uncertainty and information bias. This inverse design approach can be used with noisy data from experiments, but it is expected that the accuracy and generalisability would be affected if care is not taken to characterize the nanomaterials well (comprehensive feature extraction), and tune the RF models to accommodate the extra complexity. It is likely deeper trees would be required, and a larger number of counterfactual features would be deemed important by the forward model, making the inverse mapping more challenging.

To give an insight into how to use a trained multi-target inverse model in practice, we can consider two hypothetical instances with reasonable properties, and predict the nanoparticle that would exhibit them using each of our models. For a nanodiamond with [`Probability` =0.4, `IP` = 4.0 eV, `EA` = 3.0 eV, `EG` = 2.0 eV, `EN` = 2.5 eV] the inverse model prescribes [`sp2x`=0.04±0.016 (%), `H_conc`=0.21±0.031 (%), `sp2`=0.04±0.014 (%), `D_nm`=2.1±0.248 (nm), `FCC_conc`=0.31±0.051 (%), `CC_coord`=3.75±0.010],

with [`dCCe`=0.022±0.008 (Å), `aCCC`=109.3±0.5944 (degrees), `aCCCe`=2.1±0.7782 (degrees)] which cannot be controlled directly. Researchers in the nanodiamond community will instantly see that the fraction of sp^2-hybridized atoms, the concentration of fcc atoms, and the average carbon-carbon coordination number (for example) can be simultaneously modified using surface passivation or functionalization. For a silver nanoparticle with [`Formation_E` =0.4, `IP` = 4.0 eV, `EA` = 3.0 eV, `EG` = 2.0 eV, `EF` = −3.8 eV] the inverse model prescribes [`Ag_Ratio`=3.241±0.510, `R_avg`=7.273±1.420 (Å), `Anisotropy`=1.624±0.137, `Facets`=16.998±3.221]. The uncertainties were calculated using the MSE and are useful, as they provide researchers with a fault tolerance; essential for translation into industry. It is important to note here the different sizes (via the `D_nm` and `R_avg` metal-labels) that are required for these two nanoparticles to deliver the same `IP`, `EA`, `EG`. Additional examples for both data sets can be found in Supporting Information.

5. Conclusions

In conclusion, we have designed and demonstrated a new approach to inverse design using multi-target regression based on random forests. Using two publicly available data sets for different nanoparticles, each characterized by a set of structural features accompanied by multiple property labels, we have shown that an inverse design model that predicts a set of structural characteristics from a set of properties can have similar performance to a traditional forward model (predicting properties from the structural features) and single-target models. The inverse models are remarkably resilient against changing the number of properties of structural characteristics under consideration, but benefit computationally from restricting the structural characteristics to only those deemed important in a traditional forward structure/property model using feature importance rankings. Undertaking a precursory forward model also provides a useful indication of the approximate performance that can be expected for the inverse model, though the former is likely to be superior. This workflow is also theoretically feasible for the classification tasks as well as regression, working in concert with a multi-class classifier if the input data had discrete labels. This was outside the scope of the present study and would require further work to investigate and confirm if some kind of inverse classification is possible.

Overall the inverse design workflow used in the study is general and flexible enough to be applied to other nanoparticles and identify other types of property/structure relationships. In general, once a model that identifies a property/structure relationship is successfully trained with experimentally relevant structural features and sufficient labels, and the required accuracy, a "recipe" for nanoparticle synthesis can be predicted, taking into account the trade-offs between properties and recognizing that multi-functional nanomaterials must often meet more than one property target simultaneously. Although this model was designed for nanoparticles, there is no technical reason why it could not be applied to molecules and materials, but this would require careful consideration of how the electronic, chemical or biological features and labels were encoded. If features and labels are used that are not directly accessible then the

prediction, while numerically correct, would lack utility. It may be necessary to include techniques from interfacial informatics.[60] As it stands the workflow is entirely general, and the onus is on the user to make good decisions about how to characterize the data, how to represent their nanoparticles, molecules or materials, and how to respond to models that prescribe direct control of parameters that can only be control indirectly. Given a functional set of features and labels however, this inverse design workflow can transform design frameworks and potentially create nanomaterials suitable for multiple applications in the optical, chemical and medical domains.

Supporting Information

Supporting Information is available from the Wiley Online Library or from the author.

Acknowledgements

Conflict of Interest

The authors declare no conflict of interest.

Data Availability Statement

The data that support the findings of this study are openly available in the CSIRO Data Access repository at https://doi.org/10.25919/5ba82cf09627f, https://doi.org/10.4225/08/571F076D050B1 and https://doi.org/10.25919/5d22d20bc543e

Keywords

[1] A. Zunger, *Nat. Rev. Chem.* **2018**, *2*, 0121.
[2] B. Sanchez-Lengeling, A. Aspuru-Guzik, *Science* **2018**, *361*, 360.
[3] J. Schmidt, M. R. Marques, S. Botti, M. A. Marques, *npj Comput. Mater.* **2019**, *5*, 83.
[4] B. Sanchez-Lengeling, C. Outeiral, G. L. Guimaraes, A. Aspuru-Guzik, *ChemRxiv* **2017**. https://doi.org/10.26434/chemrxiv.5309668.v3.
[5] P. B. Jørgensen, M. N. Schmidt, O. Winther, *Mol. Inf.* **2018**, *37*, 1700133.
[6] A. Aspuru-Guzik, K. Persson, *Mission Innovation* **2018**.
[7] E. O. Pyzer-Knapp, C. Suh, R. Gómez-Bombarelli, J. Aguilera-Iparraguirre, A. Aspuru-Guzik, *Annu. Rev. Mater. Res.* **2015**, *45*, 195.
[8] A. Agrawal, A. Choudhary, *APL Mater.* **2016**, *4*, 053208.
[9] A. Aspuru-Guzik, R. Lindh, M. Reiher, *ACS Cent. Sci.* **2018**, *4*, 144.
[10] A. Barnard, B. Motevalli, A. Parker, J. Fischer, C. Feigl, G. Opletal, *Nanoscale* **2019**, *11*, 19190.
[11] A. S. Barnard, Nanodiamond data set, v1, **2016**. https://doi.org/10.4225/08/571F076D050B1 (accessed: April 2016).
[12] A. S. Barnard, Twinned nanodiamond data set, v2, **2018**. https://doi.org/10.25919/5be375f444e69 (accessed: November 2018).
[13] A. S. Barnard, B. Sun, Silver nanoparticle data set, v3, **2019**. https://doi.org/10.25919/5d22d20bc543e (accessed: July 2019).
[14] A. S. Barnard, G. Opletal, *Nanoscale* **2019**, *11*, 23165.
[15] B. Sun, M. Fernandez, A. S. Barnard, *J. Chem. Inf. Model.* **2017**, *57*, 2413.
[16] A. J. Parker, A. S. Barnard, *Nanoscale Horiz.* **2020**, *5*, 1394.
[17] N. Wagner, J. M. Rondinelli, *Front. Mater.* **2016**, *3*, 28.
[18] L. M. Ghiringhelli, J. Vybiral, S. V. Levchenko, C. Draxl, M. Scheffler, *Phys. Rev. Lett.* **2015**, *114*, 10, 105503.
[19] B. H. Menze, B. M. Kelm, R. Masuch, U. Himmelreich, P. Bachert, W. Petrich, F. A. Hamprecht, *BMC Bioinf.* **2009**, *10*, 213.
[20] A. S. Barnard, G. Opletal, S. L. Chang, *J. Phys. Chem. C* **2019**, *123*, 11207.
[21] H. Borchani, G. Varando, C. Bielza, P. Larranaga, *Wiley Interdiscip. Rev.: Data Min. Knowl. Discov.* **2015**, *5*, 216.
[22] A. Jain, G. Hautier, S. P. Ong, K. Persson, *J. Mater. Res.* **2016**, *31*, 977.
[23] H. Huo, Z. Rong, O. Kononova, W. Sun, T. Botari, T. He, V. Tshitoyan, G. Ceder, *npj Comput. Mater.* **2019**, *5*, 62.
[24] R. Caruana, A. Niculescu-Mizil, in, *Proc. of the 23rd Int. Conf. on Machine Learning*, ACM Press, New York **2006**, pp. 161–168.
[25] B. Kamiński, M. Jakubczyk, P. Szufel, *Cent. Eur. J. Oper. Res.* **2018**, *26*, 135.
[26] L. Breiman, *Mach. Learn.* **2001**, *45*, 5.
[27] L. Breiman, *Mach. Learn.* **1996**, *24*, 123.
[28] T. K. Ho, *IEEE Trans. Pattern Anal. Mach. Intell.* **1998**, *20*, 832.
[29] H. Linusson, Master's Thesis, University of Borås **2013**.
[30] C. Strobl, A.-L. Boulesteix, T. Augustin, *Comput. Stat. Data Anal.* **2007**, *52*, 483.
[31] M. R. Segal, *J. Am. Stat. Assoc.* **1992**, *87*, 407.
[32] M. Segal, Y. Xiao, *Wiley Interdiscip. Rev: Data Min. Knowl. Discov.* **2011**, *1*, 80.
[33] D. Kocev, C. Vens, J. Struyf, S. Džeroski, In *European Conference on Machine Learning*. Springer, Berlin, Heidelberg **2007**, pp. 624–631.
[34] F. Pedregosa, G. Varoquaux, A. Gramfort, V. Michel, B. Thirion, O. Grisel, M. Blondel, P. Prettenhofer, R. Weiss, V. Dubourg, J. Vanderplas, A. Passos, D. Cournapeau, M. Brucher, M. Perrot, E. Duchesnay, *J. Mach. Learn. Res.* **2011**, *12*, 2825.
[35] M. A. Razi, K. Athappilly, *Expert Syst. Appl.* **2005**, *29*, 65.
[36] D. Ho (Ed), Nanodiamonds, Springer-Verlag US, 2010, pp. 286.
[37] A. S. Barnard, *J. Phys.: Condens. Matter* **2015**, *28*, 023002.
[38] A. M. Schrand, S. A. C. Hens, O. A. Shenderova, *Crit. Rev. Solid State Mater. Sci.* **2009**, *34*, 18.
[39] V. Svetnik, A. Liaw, C. Tong, J. C. Culberson, R. P. Sheridan, B. P. Feuston, *J. Chem. Inf. Model.* **2003**, *43*, 1947.
[40] B. Ramsundar, B. Liu, Z. Wu, A. Verras, M. Tudor, R. P. Sheridan, V. Pande, *J. Chem. Inf. Model.* **2017**, *57*, 2068.
[41] A. R. Singh, B. A. Rohr, J. A. Gauthier, J. K. Nørskov, *Catal. Lett.* **2019**, *149*, 2347.
[42] A.-N. Spiess, N. Neumeyer, *BMC Pharmacol.* **2010**, *10*, 6.
[43] T. Chai, R. R. Draxler, *Geosci. Model Dev. Discuss.* **2014**, *7*, 1525.
[44] C. J. Willmott, K. Matsuura, *Clim. Res.* **2005**, *30*, 79.
[45] K. Roy, R. N. Das, P. Ambure, R. B. Aher, *Chemom. Intell. Lab. Syst.* **2016**, *152*, 18.
[46] B. Mac Namee, P. Cunningham, S. Byrne, O. I. Corrigan, *Artif. Intell. Med.* **2002**, *24*, 51.
[47] M. R. Segal, *Machine Learning Benchmarks and Random Forest Regression*, Kluwer Academic Publishers, New York **2004**.
[48] D. Tominaga, N. Koga, M. Okamoto, in, *Proceedings of the 2nd Annual Conference on Genetic and Evolutionary Computation*, ACM Press, New York **2000**, pp. 251–258.

[49] Y.-Y. Zhang, W. Gao, S. Chen, H. Xiang, X.-G. Gong, *Comput. Mater. Sci.* **2015**, *98*, 51.

[50] P. Rocca, G. Oliveri, A. Massa, *IEEE Antennas Propag. Mag.* **2011**, *53*, 38.

[51] P. Reed, B. Minsker, D. E. Goldberg, *Water Resour. Res.* **2000**, *36*, 3757.

[52] L. Yu, R. S. Kokenyesi, D. A. Keszler, A. Zunger, *Adv. Energy Mater.* **2013**, *3*, 43.

[53] D. Yang, J. Lv, X. Zhao, Q. Xu, Y. Fu, Y. Zhan, A. Zunger, L. Zhang, *Chem. Mater.* **2017**, *29*, 524.

[54] S. Dudiy, A. Zunger, *Phys. Rev. Lett.* **2006**, *97*, 046401.

[55] G. R. Schleder, A. C. Padilha, C. M. Acosta, M. Costa, A. Fazzio, *J. Phys.: Mater.* **2019**, *2*, 032001.

[56] A. Zunger, *Nature* **2019**, *566*, 447.

[57] P. Z. Hanakata, E. D. Cubuk, D. K. Campbell, H. S. Park, *Phys. Rev. Lett.* **2018**, *121*, 255304.

[58] J. Wan, J.-W. Jiang, H. S. Park, *Carbon* **2020**, *157*, 262.

[59] C. Ma, Z. Zhang, B. Luce, S. Pusateri, B. Xie, M. Rafiei, N. Hu, *npj Comput. Mater.* **2020**, *6*, 40.

[60] J. M. Fischer, A. J. Parker, A. S. Barnard, **2021**, *4*, 041001.